# A Molecular Dynamics Study of the Surfactant Surface Density of Alkanethiol Self-Assembled Monolayers on Gold Nanoparticles as a Function of the Radius

**ARTICLE** *in* THE JOURNAL OF PHYSICAL CHEMISTRY C · NOVEMBER 2010

Impact Factor: 4.77 · DOI: 10.1021/jp1088977



**4 AUTHORS:**

Alberto Jiménez-Solano
Spanish National Research Council
**11** PUBLICATIONS **30** CITATIONS
SEE PROFILE

A. Sarsa
University of Cordoba (Spain)
**91** PUBLICATIONS **1,131** CITATIONS
SEE PROFILE

Manuel Blázquez
University of Cordoba (Spain)
**76** PUBLICATIONS **883** CITATIONS
SEE PROFILE

Teresa Pineda
University of Cordoba (Spain)
**41** PUBLICATIONS **325** CITATIONS
SEE PROFILE

# A Molecular Dynamics Study of the Surfactant Surface Density of Alkanethiol Self-Assembled Monolayers on Gold Nanoparticles as a Function of the Radius

**Alberto Jiménez,[†] Antonio Sarsa,*[,†] Manuel Blázquez,[‡] and Teresa Pineda[‡]**

*Departamento de Física, Facultad de Ciencias, Edif. Albert Einstein, Planta Baja, Campus de Rabanales, Universidad de Córdoba, 14014-Córdoba, Spain, and Departamento de Química Física y Termodinámica Aplicada, Facultad de Ciencias, Edif. Marie Curie, 2ªPlanta, Campus de Rabanales, Universidad de Córdoba, 14014-Córdoba, Spain*

*Received: September 17, 2010; Revised Manuscript Received: October 27, 2010*

Atomistic molecular dynamics calculations of self-assembled monolayers of alkanethiol molecules on gold nanoparticles are carried out to determine the surface per ligand molecule as a function of the size. The molecular footprint is determined by calculating the surface tension starting from its thermodynamic definition in the canonical ensemble. We use the method of Chiu et al. (Chiu, C. C. et al. *J. Chem. Phys.* **2010**, *132*, 054706) that makes use of a parametric dependence on the system size of the potential energy between the gold surface and the ligand molecules. The role of the different groups in the molecule in the surface tension is studied. An analysis of the dependence of the surface per thiol molecule on the molecular length is carried out showing that, for molecules larger than hexanethiol, this value is independent of the number of carbon groups in the molecule. The surface occupied per molecule on spherical nanoparticles as a function of the curvature is obtained, and the method is applied to flat surfaces, obtaining a very good agreement with the experimental results. A simple model for the surface density per molecule in curved and flat surfaces is developed.

## Introduction

The study of the structural aspects and chemistry of self-assembled monolayers (SAMs) of alkanethiols on surfaces of different nature and shape is of great interest because of their potential technological applications. It is well-known that the packing density and the structure of the alkanethiol self-assembled monolayers (SAMs) depend on the nanoparticle (NP) core size[2] and are strongly influenced by the finite nature of the crystallites,[3−6] being different from those found on extended gold surfaces.[3,4,7−9] The molecular order and the packing density decrease as the distance to the particle surface increases as a consequence of increasing the available volume with the square of the radius with distance from the particle center.[10]

The structural characterization of alkanethiolate-protected gold NPs has been conducted by a combination of techniques such as high-resolution transmission electron microscopy (HR-TEM)[11,12] and small-angle X-ray scattering (SAXS)[5,6] for metal core size, NMR spectroscopy for nanoparticle size, and thermogravimetric analysis (TGA) for ligand coverage.[5,6,13−16]

Recently, some efforts have been made in the determination of the surface density of biological molecules such as DNA conjugated to gold NPs by electrospray−differential mobility analysis (ES-DMA),[17] UV−visible spectroscopy,[18] and fluorescence spectroscopy[19] techniques. In these studies, it has been found that the surface curvature significantly affects the loading of ligands with smaller particles sizes, exhibiting higher coverages than larger diameter structures. The thiol-terminated oligonucleotides attached to relatively small gold NPs (less than 20 nm diameter) show significantly more distance between the neighboring strands moving radially out from the surface than their larger particle counterparts in a way that as the nanostructures approach the molecular scale, the conformation of molecules adsorbed at their surfaces will inevitably be influenced by the nanoscale geometry.[20] Thus, the molecular conformation of the chemisorbed molecules can be strongly dependent on the surface curvature, as it has been observed for the 16-amino acid-containing peptides that change from the $\beta$-sheet conformation on 5 nm NPs to the helical structure as the curvature is reduced by increasing the core size.[21]

However, the determination of the number of ligands dotting the nanoparticle surface remains a critical technical challenge and a major barrier to commercial development. In this sense, Kalescky et al.[22] have recently reported a theoretical and computer simulation approach to calculate the surface area occupied per ligand molecule as a function of the nanoparticle radius and of the ligand hydrophobic to lipophilic balance. Starting from theoretical and molecular dynamics calculations with a coarse-grained force field. they found one order of magnitude higher ligand coverage on nanoparticles as compared to flat surfaces. Most of the theoretical studies to date consider a ligand grafting density constant, independent of the nanoparticle radius and equal to that of the same molecule on two-dimensional surfaces.[23,24] However, the packing densities of the monolayers passivating the facets of the core gold nanocrystallites differ from those found on extended gold surfaces, exhibiting organization into molecular bundles of preferred orientations which upon heating undergo a reversible melting transition near the bulk melting temperature of the alkane residue, from the ordered bundled state to a uniform intermolecular orientational distribution.[3,23] The arrangements of the molecules on such nanocrystallites are different from those found on extended surfaces and depend on the size of the nanocrystallite. In these studies, it has been found that the sulfur

* Corresponding author. Phone: +34-957-212162. Fax: +34-957-218627. E-mail: fa1sarua@uco.es.
[†] Departamento de Física.
[‡] Departamento de Química Física y Termodinámica Aplicada.

10.1021/jp1088977 
Published on Web 11/16/2010

packing densities on a crystallite of finite size with a spherical shell are about 30% or 50% larger than that on a flat extended Au(111) surface.[3,4]

In this work we present a study of the surface density of alkanethiol SAMs on gold nanoparticles as a function of the radius of curvature and on flat gold surfaces. The study is carried out by performing atomistic molecular dynamics simulations (MD). The method of Chiu et al.[1] has been adapted to our system in order to obtain the area per alkanethiolate ligand for a given nanoparticle radius.

**Methodology Force Field.** We use a force field taken from the literature.[23,25−32] The total configuration energy of the alkanethiol chains is given by

$$U = U_{\text{bond}} + U_{\text{angle}} + U_{\text{dihed}} + U_{\text{inter}} \quad (1)$$

On one hand, the intramolecular interactions are given by $U_{\text{bond}}$, $U_{\text{angle}}$, and $U_{\text{dihed}}$, which are empirical interaction functions[25−30] representing chemical bond stretching, angle bending, and torsion dihedral, respectively, and, on the other hand, the intermolecular interactions[31,32] are given by $U_{\text{inter}}$. No electrostatic interaction have been included in the intermolecular nonbonded interaction component of the force field.

In detail, the bond stretching and angle bending interactions are represented here by harmonic potentials,

$$U_{\text{bond}}(r_{ij}) = \frac{1}{2}k_r(r_{ij} - r_0)^2 \quad (2)$$

$$U_{\text{angle}}(\theta_{ijk}) = \frac{1}{2}k_\theta(\theta_{ijk} - \theta_0)^2 \quad (3)$$

while the torsion dihedral interaction is given by

$$U_{\text{dihed}}(\phi_{ijkl}) = a_0 + \frac{1}{2}[a_1(1 + \cos(\phi_{ijkl})) + a_2(1 - \cos(2\phi_{ijkl})) + a_3(1 + \cos(3\phi_{ijkl}))] \quad (4)$$

$U_{\text{inter}}$ stands for the nonbonded interactions that are modeled here as pairwise additive forces in terms of Lennard−Jones,

$$U_{\text{LJ}}(r_{ij}) = 4\varepsilon\left[\left(\frac{\sigma}{r_{ij}}\right)^{12} - \left(\frac{\sigma}{r_{ij}}\right)^{6}\right] \quad (5)$$

and a Morse potential for the Au−thiol interaction,

$$U_{\text{Morse}}(r_{ij}) = E_0[(1 - e^{-k_m(r_{ij}-r_e)})^2 - 1] \quad (6)$$

where $r_{\text{ij}}$ is the distance between atoms labeled $i$ and $j$, $\theta_{\text{ijk}}$ is the angle between the bond vectors $\vec{r}_{\text{ij}}$ and $\vec{r}_{\text{ik}}$, and $\phi_{\text{ijkl}}$ is the dihedral angle. In Table 1 we show the parameters $k_{\text{r}}$, $r_0$ $k_\theta$, $\theta_0$ $a_0$, $a_1$, $a_2$, $a_3$, $\varepsilon$, $\sigma$, $E_0$, $k_{\text{m}}$, and $r_{\text{e}}$ employed in this work.[30,32] Interaction between unlike atoms in different molecules and between the Au atoms and the atoms of the ligand molecules is calculated by using the Lorentz−Berthelot combination rules[33] starting from the Lennard−Jones parameters displayed in Table 1. The nonbonded interactions are truncated and shifted smoothly to zero at a cut off radius.

**Simulation Details.** We have carried out canonical ensemble molecular dynamics simulations for SAMs of alkanethiols ($SH(CH_2)_nCH_3$) with $n$ = 3, 5, 7, 9, 11, and 13 adsorbed on a flat Au(111) surface and on a gold nanosphere. As in similar studies,[23] the hydrogen atom of the SH headgroup is not included in the simulation. For the ligand molecules, the united atom model for the $CH_2$ and $CH_3$ groups is employed. The NPs are modeled as perfect spheres. The Au atoms are initially located randomly in the surface of the sphere at a surface density of 7.2 Å$^2$ per Au atom.[5] At zero temperature, a MD simulation is carried out to relax the Au atoms in the NP. The distance between the Au atoms and the center of the sphere is held constant in this initialization. On flat surfaces the Au atoms form a two-dimensional hexagonal lattice (111) with the same surface density as in the NP. The ligands are initialized in the all-trans configuration perpendicular to the surface at a initial distance to the surface of 2.38 Å and randomly distributed. Periodic boundary conditions in the $x$ and $y$ directions are used for the flat surface. Once equilibrated, the position of the gold atoms is held constant in the MD simulation.

**TABLE 1: Force Field Parameters**

| Bond Stretch | | |
|---|---|---|
| bond | $r_0$ (Å) | $k_{\text{r}}$ ((kcal/mol)/Å$^2$) |
| $S-CH_2$ | 1.81 | 444.00 |
| $CH_2-CH_2$ | 1.54 | 520.00 |
| $CH_2-CH_3$ | 1.54 | 520.00 |

| Angle Bend | | |
|---|---|---|
| angle | $\theta_0$ (deg) | $k_\theta$ ((kcal/mol)/rad$^2$) |
| $S-CH_2-CH_2$ | 114.40 | 125.00 |
| $CH_2-CH_2-CH_2$ | 109.47 | 126.00 |
| $CH_2-CH_2-CH_3$ | 109.47 | 126.00 |

| Torsion Dihedral | | | | |
|---|---|---|---|---|
| dihedral | $a_0$ (kcal/mol) | $a_1$ (kcal/mol) | $a_2$ (kcal/mol) | $a_3$ (kcal/mol) |
| $S-CH_2-CH_2-CH_2$ | −0.54437 | 2.8238 | 0.5437 | 6.2941 |
| $CH_2-CH_2-CH_2-CH_2$ | −0.54437 | 2.8238 | 0.5437 | 6.2941 |
| $CH_2-CH_2-CH_2-CH_3$ | −0.54437 | 2.8238 | 0.5437 | 6.2941 |

| Lennard−Jones | | |
|---|---|---|
| atoms | $\sigma$ (Å) | $\varepsilon$ (kcal/mol) |
| S−S | 4.250 | 0.397 |
| $CH_2-CH_2$ | 3.905 | 0.118 |
| $CH_3-CH_3$ | 3.905 | 0.175 |
| Au−Au | 2.935 | 0.039 |

| Morse | | | |
|---|---|---|---|
| atoms | $E_0$ (kcal/mol) | $r_{\text{e}}$ (Å) | $k_{\text{m}}$ (Å$^{-1}$) |
| S−Au | 8.76 | 2.65 | 1.47 |

The Maxwell−Boltzmann distribution corresponding to the target temperature (300 K) is employed to assign initial velocities to the ligand atoms. The NVT simulation is performed by using the Nose−Hoover thermostat. A time step of 2.0 fs is used for integrating the equations of motion. An equilibration run of 10 ns is carried out. Properties are obtained from a production run of 10 ns with configurations stored at intervals of 10 ps. We employ a cut off distance for the nonbonded potential of 10 Å. The simulations are carried out by using the DL_POLY molecular simulation package.[34]

**Calculation of the Area per Ligand.** In order to compute the optimal ligand footprint, we use the method of Chiu et al.[1] The starting point is the thermodynamics definition of the surface tension $\gamma$,

$$\gamma \equiv \left(\frac{\partial F}{\partial A}\right)_{NVT} \quad (7)$$

where $F$ is the Helmholtz free energy and $A$ is the surface area of the interface. By considering a parametric dependence of the Hamiltonian of the system in the size of the solid, $a$, the surface tension $\gamma$ can be calculated as follows,

$$\gamma = \left(\frac{\mathrm{d}A(a)}{\mathrm{d}a}\right)^{-1}\left\langle\frac{\partial U}{\partial a}\right\rangle \tag{8}$$

where $U$ is the potential energy of the system and $A(a)$ is the dependence of the surface area with the size parameter $a$. By a proper selection of the size parameter $a$, this method can be used for surfaces of arbitrary shape. The angle brackets stand for the average in the canonical ensemble in such a way that the surface tension can be obtained by computing $\langle\partial U/\partial a\rangle$ in a MD simulation.

First, this method is applied to the alkanethiolate SAMs on the NP. The NP model considered consists of Au atoms in a perfect sphere of radius $a$, so that, $\mathrm{A}(a) = 4\pi a^2$.

The potential energy, $U$, of the system depends on $a$, through interaction between the surface gold atoms and the atoms of the ligand molecules,

$$\left\langle\frac{\partial U}{\partial a}\right\rangle = \left\langle\frac{\partial}{\partial a}\sum_{i=1}^{N_{\mathrm{Au}}}\sum_{j=1}^{N_{\mathrm{lig}}} v(r_{ij})\right\rangle \tag{9}$$

where $i$ and $j$ run over all of the surface gold atoms and all of the atoms of the ligand molecules, respectively, and $v(r_{ij})$ is the interaction between the $i$ and $j$ atoms. In order to compute the derivatives, the position of the gold atoms is written as,

$$\vec{r}_i = a\hat{r}_i = a(\hat{x}_i, \hat{y}_i, \hat{z}_i)$$

Note that $\hat{r}_i$ is independent of $a$ and, $\hat{r}_i \cdot \hat{r}_i = 1$. The derivatives in eq 8 can be straightforwardly calculated, obtaining

$$\gamma = -\frac{1}{2}\frac{1}{A}\langle\sum_{i=1}^{N_{\mathrm{Au}}}\vec{F}_i\cdot\vec{r}_i\rangle, \qquad \vec{F}_i = \sum_{j=1}^{N_{\mathrm{lig}}}\left(-\frac{\mathrm{d}v(r_{ij})}{\mathrm{d}r_{ij}}\right)\frac{\vec{r}_i - \vec{r}_j}{r_{ij}} \tag{10}$$

This is an appealing expression that gives the surface tension in terms of the average of the work over the gold atoms due to the ligand molecules divided by the surface of the nanoparticle.

When the net force $\vec{F}_i$ over the $i$ gold atom is attractive, $\langle\vec{F}_i\cdot\vec{r}_i\rangle > 0$, so that $\gamma$ is negative, an expansion on the NP is induced, indicating that the grafting density is too high. The opposite holds when $\gamma > 0$ ($\langle\vec{F}_i\cdot\vec{r}_i\rangle < 0$) showing that the NP tends to contract and the grafting density is too low. The grafting density with $\gamma = 0$ will provide the optimal coverage for a given NP radius.

The same ideas can be applied to the hexagonal two-dimensional lattice considered here for flat gold surfaces. In order to compute the derivatives in eq 8, one starts by writing the coordinates of the gold atoms as follows,

$$\vec{r}_i = d\left(\left(n_i + \frac{m_i}{2}\right)\hat{x}, \frac{\sqrt{3}}{2}m_i\hat{y}\right) \tag{11}$$

where $n_i$ and $m_i$ are integers and $d$ is the nearest neighbor distance between two atoms on the Au(111) surface fixed by the value of the gold surface density. The size parameter in this case is taken as,

$$a = \sqrt{N_{\mathrm{Au}}}d \tag{12}$$

so that the surface area $A$ is

$$A(a) = \frac{\sqrt{3}}{2}a^2 \tag{13}$$

The calculation of the derivatives involved in $\gamma$, eq 8, starting from these equations leads to the same results as in the case of the NP, eq 10, with $A(a)$ given by eq 13.

For flat gold surfaces, $\langle\vec{F}_i\cdot\vec{r}_i\rangle > 0$ indicates a tendency to increase the surface so that more gold atoms are needed, i.e., the number of ligand molecules per gold atom is too high. The opposite holds for negative values of $\langle\vec{F}_i\cdot\vec{r}_i\rangle$. In terms of the surface tension we find that the surface area is too small when $\gamma$ is negative while too large values of the area lead to positive $\gamma$ values. As $\gamma$ is the derivative of the free energy with respect to the surface, eq 7, we conclude that the surface area giving $\gamma = 0$ corresponds to a minimum of the free energy.

In practice, a set of simulations with a fixed number of ligand molecules is carried out for different values of the size parameter $a$. The surface tension is calculated by using eq 10 with the corresponding $A(a)$ function. In Figure 1, the values of $\gamma$ on an NP surface as a function of $a$ for 60 tetradecanethiol molecules at 300 K are plotted. The optimum $a$ value is calculated by interpolating the results at $\gamma = 0$. The footprint is $A(a)$ evaluated at this optimum $a$ value divided by the number of ligand molecules.

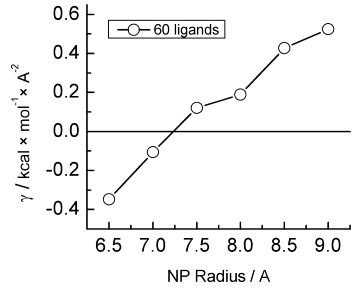


**Figure 1.** Potential of mean force on the NP as a function of NP radius for 60 tetradecanethiol molecules at 300 K.

**SCHEME 1**

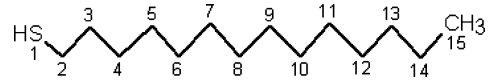


## Results and Discussion

The role of the different atoms in the tetradecanethiol ligand molecule (Scheme 1) in the $\gamma$ value is first analyzed. In doing so, the cumulative contribution to $\gamma$ as a function of the position of the group in the ligand molecule is calculated. Note that this function at the $CH_3$ terminal group gives the total surface tension.

In Figure 2, the cumulative $\gamma$ for a SAM consisting of 60 ligand molecules for two different NP radii, $R = 7.0$ Å and 7.5 Å, are plotted (the radius values are very close to the optimal NP radius of 7.2 Å, for that number of ligand molecules). The first $CH_2$ group presents a positive contribution to $\gamma$, so that on average, it lies within the repulsive core of the $CH_2-Au$

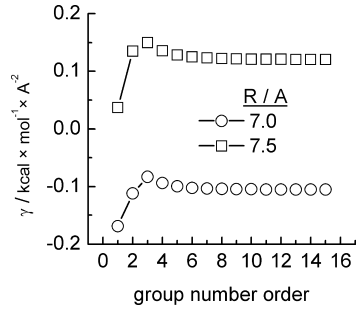


**Figure 2.** Surface tension for 60 tetradecanethiol molecules for two different NP radii at 300 K as a function of the group number (see Scheme 1 for group numbering). The optimal coverage for this system is for a NP radius of 7.2 Å.

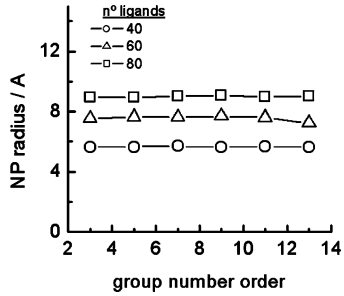


**Figure 3.** Optimal NP radius as a function of the molecular length for different number of alkanethiol molecules $S(CH_2)_nCH_3$ with $n$ = 3, 5, 7, 9, 11, 13 and different surface coverages.

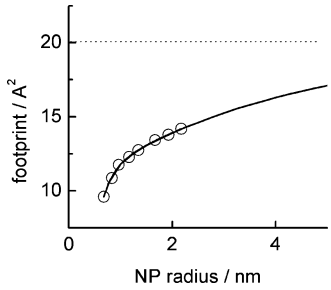


**Figure 4.** Ligand footprint as a function of the NP radius for hexanethiol molecules. The solid line is a guide to the eye.

Lennard−Jones interaction. The contribution of the rest of the $CH_2$ groups decreases as their distance to the surface increases. Because of the strong repulsion between the Au atoms and the first $CH_2$ group, the latter presents a dominant role in the optimal coverage of the NP.

The influence of the molecular length on the optimal surface density has also been studied. In doing so, different alkanethiols $SH(CH)_nCH_3$ have been considered. In Figure 3 we plot the NP radius for the molecules with $n$ = 3, 5, 7, 9, 11, and 13 and different numbers of ligands. As it is clear from these results, the optimal surface density is almost independent of the molecular length. This result is consistent with the above fact that $\gamma$ is governed by the first $CH_2$ group.

Taking into account that the optimum NP radius is almost independent of the alkanethiol length, hexanethiol molecules have been used in order to extend the present study to larger NP sizes. In Figure 4 the optimal area per surfactant as a function of the NP radius is plotted. It can be observed that for a NP radius of 2.2 nm, a footprint of around 14 Å$^2$ is obtained. This value corresponds to approximately 65% of the experimental footprint of alkanethiolates in a Au(111) two-dimensional surface.[35] In this sense, flat surfaces have also been studied by using the same methodology, fixing the number of ligands

**SCHEME 2: Area of Interaction for (a) Flat Surfaces and (b) Spherical Nanoparticles**

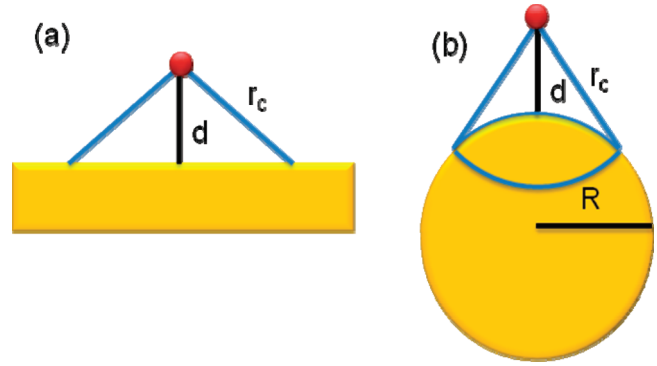


molecules to 324 and varying the number of gold atoms, obtaining a footprint of 21.2 Å$^2$ in good agreement with the experimental value of 21.6 Å$^2$.[35]

Starting from the results of the simulations performed here, a simple model for the optimal surface per ligand molecule has been elaborated. The basic assumption is that the grafting density is mainly governed by the number of gold atoms that can interact with a given ligand molecule. This number is the gold surface density times the size, $s$, of the gold surface interacting with a ligand molecule. The value of this area will strongly depend on the shape of the gold surface. We consider that the surface per ligand molecule, $\sigma$, is proportional to this area of interaction, $s$. For the sake of simplicity, to estimate $s$ a very the simple picture of the interaction of the ligand molecules with the gold surfaces studied in this work is used (Scheme 2). Thus, only those gold atom separated from a ligand molecule by an effective distance $d$ smaller than a given cut off radius, $r_c$, would interact with the molecule, and the strength of the interaction is the same for all of the Au atom such that $d \leq r_c$. For a flat surface, the value of the gold area that interacts with a molecule separated by an effective distance $d \leq r_c$, $s_F$, is readily obtained (Scheme 2a),

$$s_F = \pi(r_c^2 - d^2) \tag{14}$$

For a spherical NP of radius $R$, the size of the gold surface interacting with a ligand molecule separated by an effective distance $d \leq r_c$, $s_R$, is (Scheme 2b),

$$s_R = \pi \frac{r_c^2 - d^2}{1 + \frac{d}{R}} \tag{15}$$

The footprint in either case is proportional to these values in such a way that,

$$\frac{\sigma_R}{\sigma_F} \propto \frac{s_R}{s_F} = \frac{1}{1 + \frac{d}{R}} \tag{16}$$

where we have considered the same gold surface density for both geometries and the same interaction. In Figure 5 we plot the $\sigma_R/\sigma_F$ values as a function of the NP radius R obtained from the simulations of this work. A least-squares fitting of these values to eq 16 is carried out to fix the d value, obtaining d ≈

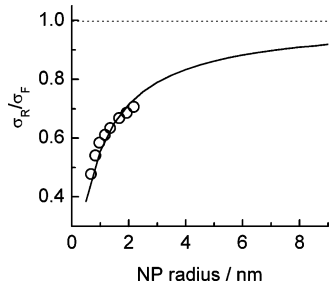


**Figure 5.** Ratio of the surface occupied by a thiol molecule in a NP and in a flat surface as a function of the NP radius calculated with the data obtained in this work (○) and from eq 16 (solid line).

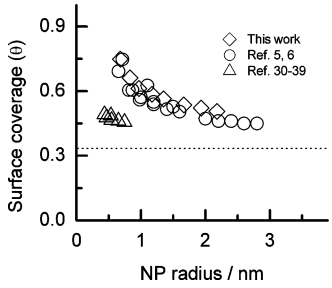


**Figure 6.** Surface coverage of alkanethiolate ligands on gold NPs as a function of the NP radius. The dotted line represents the surface coverage on flat surfaces.

0.8 nm. This analytic fit is also shown in Figure 5 as a function of the radius $R$ of the NP.

On the other hand, the comparison of the ligand coverage data obtained by Murray et al[5,6] by a combination of techniques such as high resolution-transmission electronic microscopy (HR-TEM) and thermogravimetric analysis (TGA) and taking into account the polyhedral shape of the nanoparticles gives a good agreement with the values obtained in this work (Figure 6). The preferred option to characterize metal nanoparticles in the 5−100 nm range has been HR-TEM, but this technique suffers from significant resolution problems below 3 nm. In this respect, mass spectrometry techniques have been successful to determine the exact composition of small gold NP.[36−44] Taking into account the assignments of 25, 38, 102, and 144 gold atoms nanoclusters made by this technique, it has been possible to find a correlation between the number of Au core atoms and surface thiolate ligands and on this basis assign the stoichiometry of the $Au_{68}(RS)_{34}$ cluster.[45] From these compositions, the thiolate surface coverage for these nanoclusters can be determined assuming either a sphere or a truncated octahedron shapes. The results are also displayed in Figure 6 and, as it can be observed, no good agreement has been reached.

The detailed structural characterization by X-ray crystallography have been reported for small clusters as $Au_{102}(PhCO_2H)_{44}$ and $Au_{25}(CH_2CH_2Ph)_{18}$[46,47] revealing that organothiolate ligands are not monomerically ligated to the central gold core but are instead bonded in short stellated semirings or "staples" motifs. These findings have made researchers[39] to think if the analogy of the binding mode of the thiolate ligands in nanoclusters with that in self-assembled monolayers on planar Au(111) surfaces must change to this new picture.

## Conclusions

The area per molecule of SAMs of alkanethiol molecules adsorbed on gold surfaces has been computed. The surface tension has been calculated starting from atomistic molecular dynamics calculations by using the method of Chiu et al.[1] The area per molecule is obtained by finding the surface size that provides zero surface tension for a given number of alkanethiol molecules. The surface tension is calculated as the average value in the canonical ensemble of the derivative interaction between the ligand molecules and the atoms in the surface with respect to a size parameter related to the surface. This method is adapted here to the atomistic molecular dynamics simulations of the SAMs on the Au (111) surface and spherical nanoparticles of various sizes.

For the flat surface case, we obtain a value of the area per ligand that it is in a very good agreement with the experimental value (within 1%). We have concluded that the nearest $CH_2$ group to the surface plays the most important role in the value of the surface tension. We have also determined that the value of the area per alkanethiol molecule, $SH(CH_2)_n$-$CH_3$ is roughly independent of its length, i.e., the $n$ value. A simple model is developed to relate the area per molecule in a gold NP with the area per molecule on a flat surface. The general trend is reproduced by using this model with some parameters obtained from the molecular dynamics simulations of this work.

As a conclusion, a very important parameter to understand the structure of SAM monolayers on metal substrates such as the area per molecule can be reliable when calculated by using the method here employed. The dependence of this value with the temperature or its value in mixed monolayers will be of interest. The importance of the surface density on some other structural magnitudes such as the tilt angle or the radial density needs to be elucidated.

**Acknowledgment.** We thank the Ministerio de Ciencia e Innovación (MICINN) (Projects CTQ2007-62723/BQU and FIS2009-07390) Junta de Andalucía and University of Córdoba for financial support of this work.

## References and Notes

(1) Chiu, C. C.; Ranatunga, R.; Flores, D. T.; Perez, D. V.; Moore, P. B.; Shinoda, W.; Nielsen, S. O. *J. Chem. Phys.* **2010**, *132*, 054706.
(2) Daniel, M. C.; Astruc, D. *Chem. Rev.* **2004**, *104*, 293–346.
(3) Luedtke, W. D.; Landman, U. *J. Phys. Chem.* **1996**, *100*, 13323–13329.
(4) Luedtke, W. D.; Landman, U. *J. Phys. Chem. B* **1998**, *102*, 6566–6572.
(5) Terrill, R. H.; Postlethwaite, T. A.; Chen, C. H.; Poon, C. D.; Terzis, A.; Chen, A. D.; Hutchison, J. E.; Clark, M. R.; Wignall, G.; Londono, J. D.; Superfine, R.; Falvo, M.; Johnson, C. S.; Samulski, E. T.; Murray, R. W. *J. Am. Chem. Soc.* **1995**, *117*, 12537–12548.
(6) Hostetler, M. J.; Wingate, J. E.; Zhong, C. J.; Harris, J. E.; Vachet, R. W.; Clark, M. R.; Londono, J. D.; Green, S. J.; Stokes, J. J.; Wignall, G. D.; Glish, G. L.; Porter, M. D.; Evans, N. D.; Murray, R. W. *Langmuir* **1998**, *14*, 17–30.
(7) Ulman, A. *An Introduction to Ultrathin Organic Films: From Langmuir-Blodgett to Self-assembly*; Academic Press: New York, 1991.
(8) Ulman, A. *Chem. Rev.* **1996**, *96*, 1533–1554.
(9) Dubois, L. H.; Nuzzo, R. G. *Annu. Rev. Phys. Chem.* **1992**, *43*, 437–463.
(10) Tambasco, M.; Kumar, S. K.; Szleifer, I. *Langmuir* **2008**, *24*, 8448–8451.
(11) Brust, M.; Walker, M.; Bethell, D.; Schiffrin, D. J.; Whyman, R. *J. Chem. Soc., Chem. Commun.* **1994**, 801–802.
(12) Brust, M.; Fink, J.; Bethell, D.; Schiffrin, D. J.; Kiely, C. *J. Chem. Soc., Chem. Commun.* **1995**, 1655–1656.
(13) Corbierre, M. K.; Cameron, N. S.; Lennox, R. B. *Langmuir* **2004**, *20*, 2867–2873.
(14) Fabris, L.; Antonello, S.; Armelao, L.; Donkers, R. L.; Polo, F.; Toniolo, C.; Maran, F. *J. Am. Chem. Soc.* **2006**, *128*, 326–336.
(15) Kim, B. J.; Fredrickson, G. H.; Kramer, E. J. *Macromolecules* **2008**, *41*, 436–447.
(16) Viudez, A. J.; Madueno, R.; Blazquez, M.; Pineda, T. *J. Phys. Chem. C* **2009**, *113*, 5186–5192.
(17) Pease, L. F.; Tsai, D. H.; Zangmeister, R. A.; Zachariah, M. R.; Tarlov, M. J. *J. Phys. Chem. C* **2007**, *111*, 17155–17157.
(18) Kira, A.; Kim, H.; Yasuda, K. *Langmuir* **2009**, *25*, 1285–1288.

(19) Hill, H. D.; Millstone, J. E.; Banholzer, M. J.; Mirkin, C. A. *ACS Nano* **2009**, *3*, 418–424.
(20) Weeraman, C.; Yatawara, A. K.; Bordenyuk, A. N.; Benderskii, A. V. *J. Am. Chem. Soc.* **2006**, *128*, 14244–14245.
(21) Mandal, H. S.; Kraatz, H. B. *J. Am. Chem. Soc.* **2007**, *129*, 6356–6357.
(22) Kalescky, R. J. B.; Shinoda, W.; Moore, P. B.; Nielsen, S. O. *Langmuir* **2009**, *25*, 1352–1359.
(23) Ghorai, P. K.; Glotzer, S. C. *J. Phys. Chem. C* **2007**, *111*, 15857–15862.
(24) Leff, D. V.; Ohara, P. C.; Heath, J. R.; Gelbart, W. M. *J. Phys. Chem.* **1995**, *99*, 7036–7041.
(25) Weiner, S. J.; Kollman, P. A.; Case, D. A.; Singh, U. C.; Ghio, C.; Alagona, G.; Profeta, S.; Weiner, P. *J. Am. Chem. Soc.* **1984**, *106*, 765–784.
(26) Li, Y. Y.; Lin, S. T.; Goddard, W. A. *J. Am. Chem. Soc.* **2004**, *126*, 1872–1885.
(27) Alexiadis, O.; Harmandaris, V. A.; Mavrantzas, V. G.; Delle Site, L. *J. Phys. Chem. C* **2007**, *111*, 6380–6391.
(28) Bocker, J.; Schlenkrich, M.; Bopp, P.; Brickmann, J. *J. Phys. Chem.* **1992**, *96*, 9915–9922.
(29) Jorgensen, W. L.; Madura, J. D.; Swenson, C. J. *J. Am. Chem. Soc.* **1984**, *106*, 6638–6646.
(30) Jorgensen, W. L.; Maxwell, D. S.; TiradoRives, J. *J. Am. Chem. Soc.* **1996**, *118*, 11225–11236.
(31) Hautman, J.; Klein, M. L. *J. Chem. Phys.* **1989**, *91*, 4994–5001.
(32) Zhao, X. C.; Leng, Y. S.; Cummings, P. T. *Langmuir* **2006**, *22*, 4116–4124.
(33) Allen, M. P.; Tildesley, D. J. *Computer Simulation of Liquids*; Clarendon Press: Oxford, 1987.
(34) Smith, W.; Forester, T. R.; Todorov, I. I. *The DL_POLY2 user manual*; STFC Daresbury Laboratory: Cheshire, UK, 2009.
(35) Mar, W.; Klein, M. L. *Langmuir* **1994**, *10*, 188–196.
(36) Whetten, R. L.; Khoury, J. T.; Alvarez, M. M.; Murthy, S.; Vezmar, I.; Wang, Z. L.; Stephens, P. W.; Cleveland, C. L.; Luedtke, W. D.; Landman, U. *Adv. Mater.* **1996**, *8*, 428.
(37) Schaaff, T. G.; Knight, G.; Shafigullin, M. N.; Borkman, R. F.; Whetten, R. L. *J. Phys. Chem. B* **1998**, *102*, 10643–10646.
(38) Schaaff, T. G.; Whetten, R. L. *J. Phys. Chem. B* **2000**, *104*, 2630–2641.
(39) Dass, A.; Dubay, G. R.; Fields-Zinna, C. A.; Murray, R. W. *Anal. Chem.* **2008**, *80*, 6845–6849.
(40) Negishi, Y.; Nobusada, K.; Tsukuda, T. *J. Am. Chem. Soc.* **2005**, *127*, 5261–5270.
(41) Tracy, J. B.; Crowe, M. C.; Parker, J. F.; Hampe, O.; Fields-Zinna, C. A.; Dass, A.; Murray, R. W. *J. Am. Chem. Soc.* **2007**, *129*, 16209–16215.
(42) Tracy, J. B.; Kalyuzhny, G.; Crowe, M. C.; Balasubramanian, R.; Choi, J. P.; Murray, R. W. *J. Am. Chem. Soc.* **2007**, *129*, 6706–+.
(43) Dass, A.; Stevenson, A.; Dubay, G. R.; Tracy, J. B.; Murray, R. W. *J. Am. Chem. Soc.* **2008**, *130*, 5940–5946.
(44) Qian, H. F.; Jin, R. C. *Nano Lett.* **2009**, *9*, 4083–4087.
(45) Dass, A. *J. Am. Chem. Soc.* **2009**, *131*, 11666–11667.
(46) Jadzinsky, P. D.; Calero, G.; Ackerson, C. J.; Bushnell, D. A.; Kornberg, R. D. *Science* **2007**, *318*, 430–433.
(47) Heaven, M. W.; Dass, A.; White, P. S.; Holt, K. M.; Murray, R. W. *J. Am. Chem. Soc.* **2008**, *130*, 3754–3755.

JP1088977